PROJECT 3269
FEB 11 '76 Rept 1

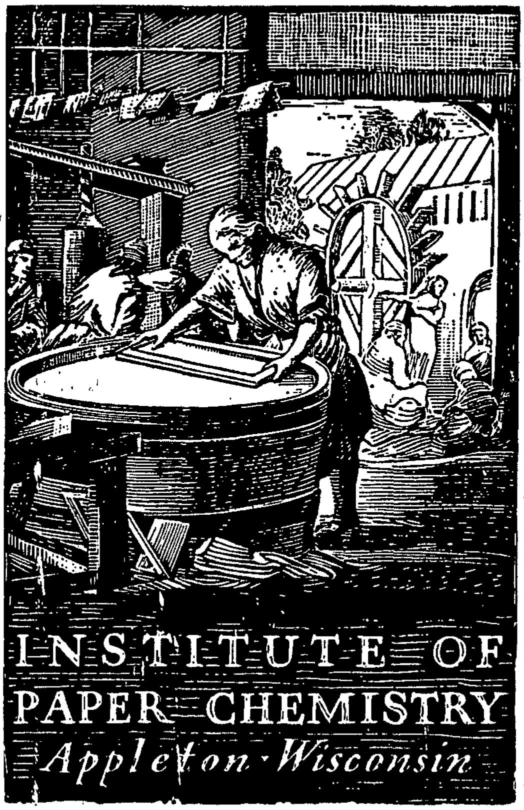

DEVELOPMENT OF MEANS FOR MEASURING THE EFFECT OF SURFACE FINISH ON PRINT QUALITY

Project 3269
2

Report One

A Progress Report

to

MEMBERS OF THE INSTITUTE OF PAPER CHEMISTRY

January 12, 1976

THE INSTITUTE OF PAPER CHEMISTRY

Appleton, Wisconsin

DEVELOPMENT OF MEANS FOR MEASURING THE EFFECT OF SURFACE FINISH ON PRINT QUALITY

Project 3269

Report One

A Progress Report

to

MEMBERS OF THE INSTITUTE OF PAPER CHEMISTRY

January 12, 1976

TABLE OF CONTENTS

THE INSTITUTE OF PAPER CHEMISTRY

Appleton, Wisconsin

DEVELOPMENT OF MEANS FOR MEASURING THE EFFECT OF SURFACE FINISH ON PRINT QUALITY

SUMMARY

The light which is reflected from a printed paper is of two types. The portion which is transmitted by the ink film and scattered back through the ink film by the paper is modified in both intensity and wavelength distribution by the ink pigment. However, another portion of the incident light is reflected from the upper surface of the ink with little or no change caused by the colorants which are within the ink film. The color saturation or purity of the print depends upon how well the observer is able to avoid the surface component of the reflected light. If the surface is highly glossy this surface component is largely confined to the specular angle and can be avoided by adjustment of viewing conditions. The angular distribution of the surface reflection depends upon the finish of the inked surface which in turn is dependent upon the surface properties of the paper substrate. Since the amount of color degradation is a direct function of the amount of surface reflection occurring at the viewing angle, a logical means of evaluating the potential color printing quality of papers would be to measure the surface component of reflected light at the viewing angle under normal viewing conditions.

As the first step in this investigation, a colorimeter has been devised for measuring the color characteristics of both the surface and internal components of the light reflected at a viewing angle of 0° and variable angle of incidence. This resolution into components is accomplished by using polarized incident light and relying on the depolarization of internally scattered light but reflection without depolarization from the surface. Color measurement is accomplished by

use of filters which, in combination with light source and photoreceptor, provide reflectance factors closely approximating the $R_{X(red)}$, R_Y and R_Z functions of the CIE system. The $R_{X(blue)}$ reflectance factor is approximated by R_Z. In preliminary tests of printed papers the normally observed composite color has been resolved into the more saturated color of the internal component and a much less saturated near white due to surface reflection. The selective surface reflection known as "bronzing" which is commonly found with red prints was detected by the desaturated yellow-orange hue of its surface component. In all cases the degrading effect of the surface reflection could be quantitatively evaluated.

Now that adequate means of measurement are available, the next step in the program will be the comparison of prints made with the same quantity of ink on a variety of coated and uncoated papers. The potential color printing quality of the papers will be evaluated from the colorimetric data. However, correlation with less complicated measurements, such as an achromic determination of surface reflectance factor at a single incident angle, which might be used routinely by the papermaker, will be investigated.

INTRODUCTION

Experiments in which a constant amount of ink has been printed on different papers have shown that the color of the printed surface can be highly dependent upon the paper used. Some of the differences may be ascribed to the color of the paper or to the penetration of ink to a depth where it is not as effective, but the "finish" or roughness on a submicroscopic scale is also important. To account for the effect of finish it is necessary to consider all of the light coming from the printed surface which enters the eye of the observer. This light is composed of image and nonimage components. The image component has been modulated in intensity and wavelength distribution by transmission through the ink film, by scattering within the paper substrate, and by retransmission back through the inked surface. The nonimage light has been reflected from the upper surface of the ink film essentially without absorption by the colorants which are within the film. As a result, the image light is diluted with nonimage white light in a manner which is analogous to that occurring when ambient light falls on the screen during the projection of color transparencies. Colors are desaturated and lightened and the maximum density and attainable contrast are restricted.

The image light coming from beneath the printed surface emerges with a spatial distribution approximating the spherical distribution described by Lambert's Cosine Law. This distribution is essentially independent of either the incident angle or the surface finish. Consequently, the printed image may be viewed from any angle although viewing along the normal to the surface is strongly preferred because image light is greatest in this direction and because the visual image is undistorted by the forshortening which occurs with oblique viewing. However, the spatial distribution of the nonimage surface reflection is strongly dependent upon the finish of the surface. If the surface is glossy, this nonimage component is so strongly concentrated in the region of the specular angle that the viewer can avoid it by choice of viewing conditions. However, if the print has a matte surface the undesired surface reflection is so widely distributed that there is no viewing geometry by which it can be avoided.

It should be noted that the detrimental effects of surface reflection upon the appearance of a print are greatest in the blackest blacks and most saturated colors. In contrast, the surface reflection has a small but beneficial effect upon the lightness of whites. Therefore, the optimum surface finish condition should be attained when a nonglossy paper capable of high printed ink gloss is used. Unfortunately, the view that high paper gloss is required to achieve high print gloss is widely held.

Printed gloss is commonly accepted as a satisfactory measure of the desirable surface finish which permits the viewer to see the printed image at maximum color saturation and contrast with the least interference by surface reflection. It is at best an indirect measure. It is assumed that the amount of reflected light found at the specular angle in the gloss determination is a reliable indicator of the absence of surface reflection at normal viewing angles under actual viewing conditions. However, gloss measurements are commonly made at 75° incidence even though prints are rarely viewed with any substantial portion of the light incident at such a large angle. The size of surface irregularities which can be tolerated without affecting gloss increases strongly with increasing incident angle. Furthermore, the gloss value does not provide reliable information concerning the spatial distribution of nonspecular surface reflection. This is particularly evident in the case of textured or embossed papers which have low gloss but sometimes provide prints of high color saturation. For these reasons the reliability of using paper gloss and printed ink gloss as measures of the suitability of a paper where high printing quality is demanded must be highly suspect. A method is needed by which the papermaker can measure printed and unprinted surface reflectance at viewing angles for realistic conditions of illumination.

Direct measurement of surface reflection at viewing angles requires a means for distinguishing between the light reflected from the surface and that coming from beneath the surface. A method for doing this, which depends upon the depolarization of internally scattered light and the reflection without depolarization from the surface, has been reported by the Institute (1). Although this technique was originally used to explore the distribution of surface reflection in the region surrounding the specular angle, it is also suitable for determination of surface reflection along the normal to the surface for the range of incident angles which are likely to be used in viewing prints. The same method can be used for prints, where the surface reflection is undesirable, and for unprinted papers, where surface reflection is somewhat beneficial. The possibility of converting the measuring instrument into a colorimeter permits the quantitative determination of the effect of surface reflection upon color in terms that can be expressed as visual color difference.

OBJECTIVES

The objectives of this research are:

1. Development of a direct method of measurement by which the printing quality characteristics now associated with paper and printed gloss can be objectively determined.
2. Determination of the extent to which printed surface reflectance characteristics provided by papers of low gloss are compatible with the high contrast range and color saturation associated with high printed gloss.
3. Specification of the type of abridged instrument needed for routine measurements of the surface reflectance characteristics of papers and prints, to be based on the particular measurements which prove to be most significant.

DISCUSSION OF THE PROBLEM

The intensity of surface reflection, I_F, from a dielectric surface is related to the incident intensity, I_o, the angle of incidence, i, and the refractive index, n, by the Fresnel Equation, which may be written in the form

$$\frac{I_F}{I_o} = \frac{1}{2}\left[\frac{(\cos i - \sqrt{n^2 - \sin^2 i})^2}{(\cos i + \sqrt{n^2 - \sin^2 i})^2} + \frac{(n^2\cos i - \sqrt{n^2 - \sin^2 i})^2}{(n^2\cos i + \sqrt{n^2 - \sin^2 i})^2}\right]. \qquad (1)$$

For an optically smooth surface this surface reflection is at the specular angle, equal and opposite the incident angle. Imperfectly smooth surfaces with surface reflection largely near the specular angle are described as glossy and those with widely scattered surface reflection are described as having matte surfaces. It is the surface reflection at the nonspecular viewing angle which limits the color saturation and contrast of printed images. However, it is usually assumed that high gloss correlates with low surface reflectance at nonspecular angles, even though the gloss measurement actually provides no information concerning the distribution of the remaining surface reflection over nonspecular angles.

Some information concerning the size of surface irregularities affecting gloss is provided by Equation (2) which has been discussed by Depew and Weir (2).

$$I_S/I_F = \exp - \left[\frac{4\pi\ \sigma\ \cos i}{\lambda}\right]^2 + \left[\frac{2^5\ \pi^3}{m^2}\ \left(\frac{\sigma}{\lambda}\right)^4\ \cos i^3\ \Delta\omega\right] \qquad (2)$$

In this equation I_S is the surface reflectance, I_F is the Fresnel reflection of Equation (1), σ is the standard deviation in surface elevation from the mean plane, m is the standard deviation of surface slope, λ is the wavelength of light, and $\Delta\omega$ is the solid angle accepted by the receptor. The first term in this equation describes the reduction in specular intensity due to scattering by diffraction effects. The second term is due to the spreading of light caused by reflection from facets which are inclined to the nominal plane of the surface. The ratio $\underline{I_S}/\underline{I_F}$ has been called the surface reflectance factor, SRF, (3). SRF × 100 can be considered substantially equivalent to percent gloss. It differs only in that the reference material is an optically smooth surface of the same material rather than an arbitrary glass standard.

When σ is small relative to λ and $\Delta\omega$ is small, the second term in Equation (2) becomes negligible and the equation reduces to

$$I_S/I_F = \exp - \left[\frac{4\pi\ \sigma\ \cos\ i}{\lambda}\right]^2 \qquad (3)$$

A plot of SRF vs. σ/λ for several angles of incidence, as calculated from Equation (3) is shown as Fig. 1. It will be evident from this plot that a root mean square unevenness, σ, of 50% of the wavelength of light is sufficient to reduce the SRF to less than 10% even at 75° incidence. At λ = 550 nm, the median wavelength of the visible spectrum, this is an unevenness of less than 0.3 µm. An ink film of approximately 2.0 µm in thickness should completely cover such paper surface irregularities and produce a new surface which is not affected by the texture of the substrate. Therefore, there seems to be no reason why paper gloss should be a necessary requirement for the attainment of printed ink gloss.

It is possible that a rougher paper might have an appreciable SRF due to reflection from surface elements which are inclined from the surface plane in the manner described by the second term in Equation (2). Gate, Highman and Hine (4) have estimated that a surface having a mean inclination of 8° with peak to valley depths and lateral distances of 2 and 50 µm, respectively, should have a gloss of about 10%. Even in this case a 2 µm ink film would have ample volume to fill the valleys and produce a surface much smoother than the substrate.

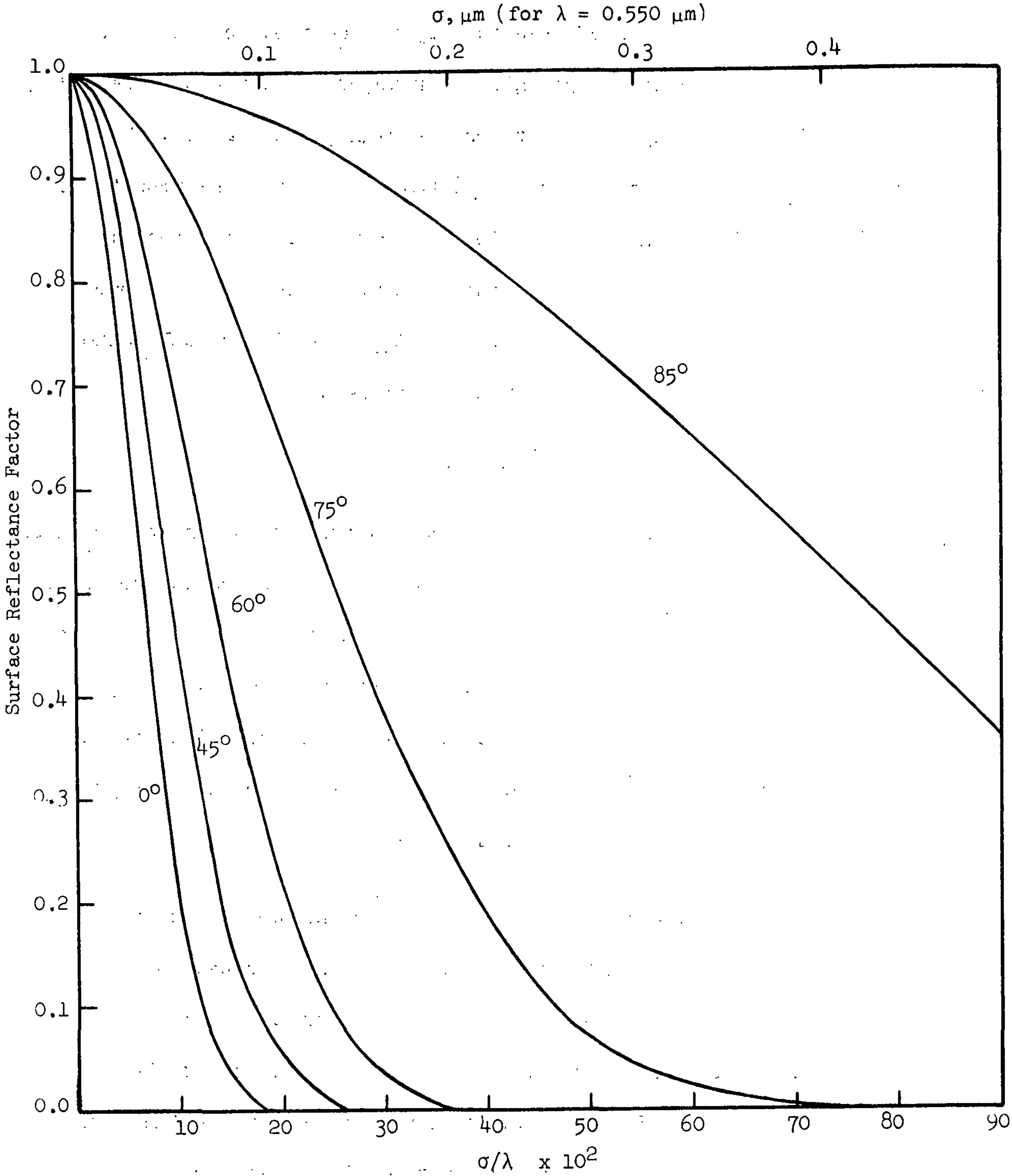

Figure 1. Surface Reflectance Factor (SRF) Calculated from the Equation

$$SRF = \exp - \left[\frac{4\ \sigma \cos i}{\lambda}\right]^2$$

as a Function of σ/λ for Selected Angles of Incidence

The above arguments are offered to support the view that high ink gloss does not necessarily require high paper gloss. However, it can not be denied that most present low gloss papers do not produce high printed gloss. Workers at the Graphic Arts Technical Foundation (5,6) have recognized the importance of those paper properties which enhance ink gloss and have proposed a quantity "paper surface efficiency," PSE, as a measure of the ink gloss potential of a paper surface and its suitability for color printing. PSE is a linear combination of paper gloss and ink receptivity defined by the expression

$$PSE = \frac{(100-A) + PG}{2}$$

where PG is the 75° paper gloss and A is the ink absorptivity of the paper which is obtained by measuring the reflectance of K&N ink stain. There can be no doubt that the PSE provides a qualitative relationship for predicting ink gloss that seems to apply to many papers but some exceptions have been noted. The PSE has not been widely adopted — probably because it fails to reliably differentiate between similar papers. Furthermore, there seems to be little need for prediction of 75° printed gloss which can be easily determined.

The use of printed gloss as a measure of the suitability of paper for prints of high color saturation and contrast may be criticized because of the indirect nature of the test. The degree of absence of surface reflection at viewing angles must be inferred from a large concentration of the reflected light at the specular angle. However, nothing is known concerning the angular distribution of the nonspecular component. In view of the two mechanisms for dispersion of surface reflection which are considered in Equation (2) this distribution may be expected to vary with the surface characteristics of the paper. Furthermore, the use of 75° incidence for gloss measurements compounds this uncertainty in view of the large effect of angle of incidence illustrated in

Fig. 1. Certainly prints are rarely viewed with any substantial portion of the illumination incident at such a large angle. Furthermore, reliance upon ink gloss may result in a demand for gloss which extends beyond the point at which any real quality advantage can be shown.

In view of serious questions concerning the reliability of specular gloss measurements for indication of the degree to which surface reflection is absent at nonspecular viewing angles, it would be desirable to have a method, based on reasonable conditions for viewing prints, for determining the amount of undesired surface reflectance at the viewing angle. This surface reflectance must be determined in the presence of image light scattered from the interior of the print so a means of distinguishing between surface and internal reflection is required. Such a method was devised by Leekley, Denzer and Tyler (1) for study of the components of reflectance in the region of the specular peak. More recently, a similar method has been employed by Bryntse and Norman (7). The sample is illuminated with plane polarized light and viewed with a receptor which contains a polarizing analyzer. Light from the interior of the print is depolarized by scattering but light is reflected from the surface without depolarization. Therefore, the flux of internally reflected light is twice that found when the analyzer accepts light polarized perpendicularly to the incident light. The surface flux is the difference between that found with the analyzer in the parallel and perpendicular orientations.

The above method was adopted for the present study of the internal and surface reflectance at a viewing angle of 0° and variable angle of incidence. It was decided to modify the equipment used previously (1) to include filters for color measurement in the CIE system. This would permit the evaluation of the magnitude of effect of surface difference in terms of visual color difference.

It is not expected that actual color measurement will be required if an instrument is eventually designed for routine use.

DESIGN OF THE EQUIPMENT

BASIC DESIGN

The goniophotometer which was used previously (1) was modified for the present work. No changes other than the introduction of color filters were anticipated. However, because of the low light level, particularly when the filters were introduced, a number of other changes were required which are described in the following paragraphs.

INCIDENT LIGHT SOURCE

The light source which was used in the previous work (1) was reconstructed in order to increase the amount of light. The design is shown schematically in Fig. 2. The filament of the lamp (General Electric No. 1962) is imaged by the condensing lens L_1 at the aperture A_1. Light passing through the Rochon prism P_1 is resolved into ordinary (axial) and extraordinary (nonaxial) beams which are polarized in planes which are perpendicular to one another. Consequently, the lens L_2 forms two nonoverlapping images of aperture A_1 in the plane of aperture A_2. Aperture A_2 accepts the ordinary beam and rejects the extraordinary beam. The lens L_3 projects an image of the entrance aperture of the Rochon prism (A_3) which is in focus at the center of the specimen. At focus the beam has a diameter of 9/16 inch. The effective half angle of the beam, as limited by aperture A_4 at the projection lens is $3.5°$. Therefore, each point on the specimen is illuminated through a solid angle of 0.012 steradian.

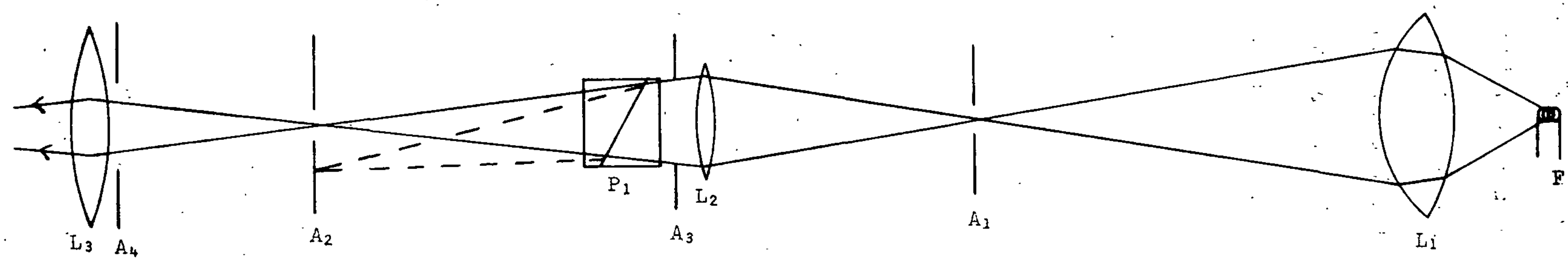

Figure 2. Schematic Diagram of the Light Source. A_1, A_2, A_3, and A_4 are Apertures, L_1, L_2, and L_3 are Lenses, F is the Lamp Filament and P_1 is the Rochon Prism. The Extraordinary Beam is Indicated by Dotted Lines

The angle of polarization is controlled by rotation of the Rochon prism within the optical system. The handle by which it is rotated travels between stops at which the polarization is either parallel or perpendicular to the plane containing the incident and specular beams. The whole light source is mounted on a circular track which permits change in the angle of incidence without changing the point at which the axis of the beam intersects the plane of the specimen.

The lamp is operated at 6.0 volts d.c. using a Lambda model LK 340 regulated power supply. A fiber optic is mounted in the lamp housing to sample the lamp intensity and provide a reference beam against which the intensity of light reflected by the specimen is compared.

RECEPTOR OPTICAL SYSTEM

The optical system used for the receptor is similar to that used for the light source and is shown schematically in Fig. 3. The specimen surface is imaged by the objective lens L_4 upon aperture A_5 which limits the field of view. Ordinary and extraordinary beam images of A_4 are formed in the plane of aperture A_5 by lens L_5 through the Rochon prism P_2. The ordinary beam passes through the aperture A_6 to the photoreceptor R but the extraordinary beam is excluded by the aperture plate. The receptor optical system is mounted in a fixed position with its axis perpendicular to the central point of the specimen area which is illuminated by the light source. The plane of polarization accepted by the receptor is controlled by rotation of the whole optical system about its own axis. Stops are provided for adjusting to accept light polarized either parallel or perpendicular to the plane containing the incident and specular beams. The specimen area viewed by the receptor, as checked by back projection of light through the optical system, is 3/8 inch in diameter and is centered in the eliptical illuminated area of the specimen which has a minor

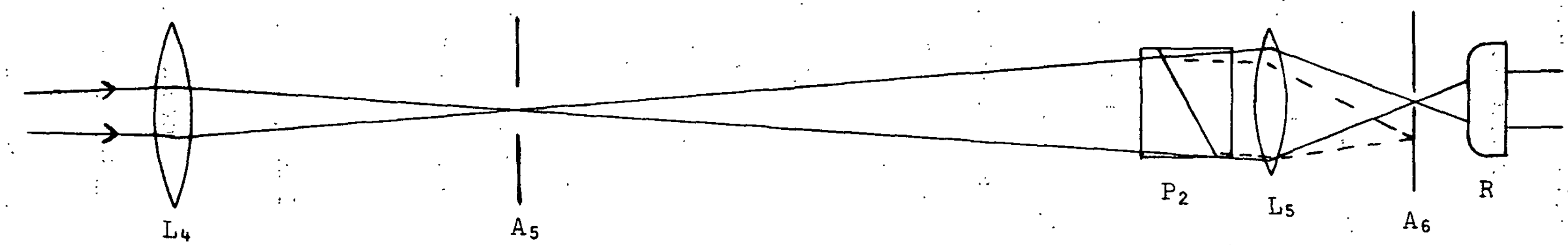

Figure 3. Schematic Diagram of the Receptor Optical System. A_5 and A_6 are Apertures, L_4 and L_5 are Lenses, P_2 is the Rochon Prism, and R is the Photoreceptor. The Extraordinary Beam is Indicated by Dotted Lines

diameter of 9/16 inch. The half angle of the receptor, as determined from the beam diameter at lens L_4 during back projection is 1.6° which corresponds to a solid angle of 0.0024 steradian.

The color filters are inserted in a slotted collar which extends beyond lens L_4 and which is not shown in the diagram.

LIGHT DETECTION AND MEASUREMENT

An attempt was made to use the photomultiplier photometer (Densichron Model 400) and digital voltmeter which was used in the previous work (1). However, the stability of the readings was not satisfactory. An attempt was then made to use silicon photocells (United Detector Technology, PIN-10) but the level of light available proved to be too low. Therefore, two photoconductive cells (Clairex CL 505L) are used in the bridge circuit shown schematically in Fig. 4. The reference cell ($R_{\lambda\ ref}$) is illuminated through a fiber optic by light from the light source while the other cell (R_λ) detects the light which is reflected by the specimen and transmitted by the receptor optical system. The resistances R_1, R_2, R_3, and R_4 are 0 to 999.9 ohm decade boxes (Leeds and Northrop 4776). The imbalance of the bridge is detected by a sensitive mirror galvanometer (Rubicon 3414) which is operated at varying sensitivity by means of a galvanometer shunt. At balance,

$$\frac{R_1 + R_2}{R_3 + R_4} = \frac{R_{\lambda\ ref}}{R_\lambda}$$

and, because the resistance of the photoconductors is inversely proportional to the corresponding light intensities, I and I_{ref},

$$\frac{R_1 + R_2}{R_3 + R_4} = \frac{I}{I_{ref}} .$$

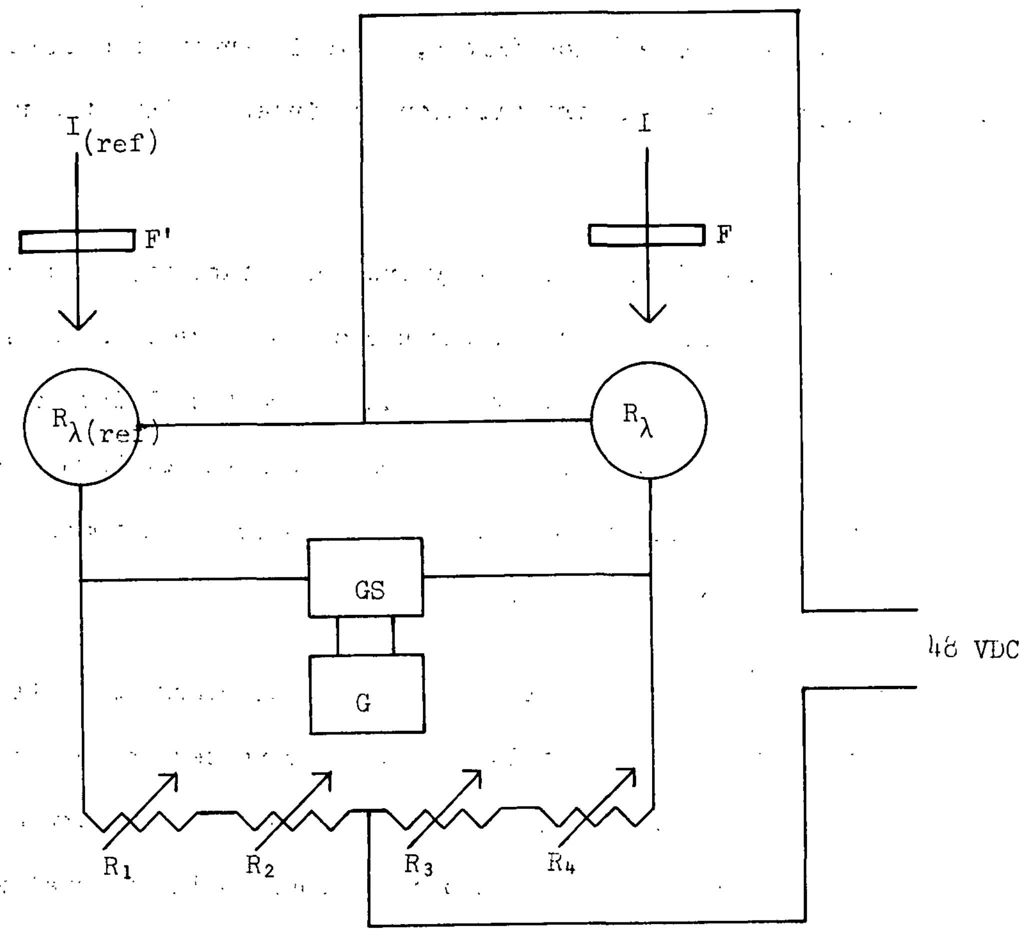

Figure 4. Schematic Diagram of Light Measuring System. $\underline{R}_\lambda$ and $\underline{R}_{\lambda\ ref}$ are Photoconductive Cells Illuminated by the Light Reflected by the Specimen, $\underline{I}$, and the Reference Beam, $\underline{I}_{ref}$, Respectively. $\underline{F}$ is a Colorimetric Filter and $\underline{F}'$ is a Dummy Filter Which Keeps the Light Level on the Photoconductors in the Same Range. $\underline{R}_1$, $\underline{R}_2$, $\underline{R}_3$, $\underline{R}_4$ are 0 to 999.9 Ohm Decade Boxes, $\underline{GS}$ is a Galvanometer Shunt and $\underline{G}$ a Galvanometer

Therefore, at balance, the digital resistance, $\underline{R}_1 + \underline{R}_2$, read from the dials of the decade boxes is proportional to the specimen reflectance. The resistances $\underline{R}_3$ and $\underline{R}_4$ are used to adjust the readings of $\underline{R}_1 + \underline{R}_2$ to predetermined values using standards of known reflectance. Small changes in the intensity of the light source should be compensated by like changes in the intensity of the reference beam. It is necessary that the intensities $\underline{I}$ and $\underline{I}_{ref}$ be of the same magnitude. Therefore, when a color filter, F, is inserted into the receptor beam, another filter, F', of similar transmission is inserted into the reference beam.

The system has shown high sensitivity and good stability. Balance can be read to the closest tenth ohm. However, the photoconductive cells do have a "memory" for their recent light history. This requires waiting before a stable balance is attained. The time required depends upon the level of light being measured. This would not be satisfactory for making routine measurements but it can be tolerated in a research instrument.

It should be noted that the cells have a voltage memory as well as a light memory. Initially the two photoconductors were connected in series in the expectation that it might be an advantage if both carried the same current when the bridge was balanced. Under these conditions a change in light level at either cell caused a change in voltage drop across both cells and much more time was required to achieve equilibrium.

CONVERSION OF THE REFLECTOMETER TO A THREE FILTER COLORIMETER

To provide for measuring color it was necessary to select color filters which in combination with the spectral distribution of the light source and the spectral sensitivity of the photoreceptor would provide instrument responses approximating the X (red portion), Y, and Z responses of the CIE system. Evaluation of the three filter combinations was accomplished by the method devised by Van den Akker and Dearth (8) who selected a series of colored glass filters for use in calibration of filter colorimeters. For each calibration filter there is a corresponding clear glass blank of similar thickness and refractive index which is used to eliminate effects due to surface reflection and change in optical path length. At least four calibration filters are used for each function. Two filters with spectral transmission curves which are nearly linear across the full band of the function, each transmitting about half of the energy of the function, but one with a positive and one with a negative slope, are used to establish the effective wavelength of the response. Sharp cutting filters which transmit in the extremes of the band are used to provide a measure of the breadth of the response. The transmittance of these calibration filters has been determined on a spectrophotometer which was itself calibrated by the method of Van den Akker (9). For each filter, integrations have been performed to determine the required CIE response associated with substitution of the filter for the corresponding blank.

The method of tailoring the instrument filters to the desired responses was one of trial and error. The extent to which X (red portion), Y, and Z responses of the instrument meet the required values for the calibration filters with the instrument filters which were finally selected is shown in Table I. Further information concerning the color characteristics of the components of this system is included in Appendix I. The individual filter elements comprising the instrument filters are listed in Table IV. Transmittance curves for the three composite filters are shown as Fig. 7.

The instrument responses are governed by the spectral sensitivity of the photoconductive cell and the energy distribution of the quartz-iodine lamp as well as by the spectral transmittance of the filters. In the absence of an experimentally determined sensitivity curve for the photoconductive cell, a curve prepared from representative data supplied by the manufacturer is included as Fig. 8.

TABLE I

INSTRUMENT RESPONSE TO CALIBRATION FILTERS

Calibration Filter	Response, % Required	Found	Error
	R_X(red)		
S (brown)	49.0	48.9[a]	-0.1
U (blue)	48.2	47.4[a]	-0.8
V (blue)	14.4	14.9[a]	+0.5
Y (red)	18.4	18.4[a]	0.0
Z (red)	2.0	3.3[a]	+1.3
	R_Y		
R (brown)	60.4	60.2[a]	-0.2
V (blue)	68.3	68.4[a]	+0.1
W (blue)	25.8	23.5[a]	-2.3
X (red)	24.6	20.9[a]	-3.7
Y (red)	5.8	4.8[a]	-1.0
	R_Z		
A (green)	48.0	48.4	+0.4
B (blue)	55.8	56.6	+0.8
C (green)	7.0	6.4	-0.6
D (blue)	14.6	14.3	-0.3

[a]The values shown are corrected for photometric nonlinearity by the method described in the following section.

DETERMINATION OF PHOTOMETRIC LINEARITY

The photometric linearity was determined by the addition of light fluxes essentially as described by Höpert and Loof (10). The method requires that an auxilliary light source of variable intensity be used in addition to the regular light source. Therefore, a source equipped with two variable density wedges was provided. The instrument was adjusted to require a resistance of 1000 ohms when the $BaSO_4$ compact was illuminated with the regular light source. The intensity of illumination was then reduced by placing a screen of nominally 29.1% transmission over the regular light source. This new level was arbitrarily assigned an intensity, $\underline{I} = 1.0$ and the required resistance was determined. Light from the regular light source was then blocked and the auxilliary light source was adjusted to an intensity $\underline{I} = 1.0$ as judged by balance at the same resistance. Next the standard was illuminated simultaneously by both light sources to provide an intensity, $\underline{I} = 2.0$, and the resistance required for balance was again determined. The light from the regular source was then blocked again and the intensity of the auxilliary source adjusted to $\underline{I} = 2.0$. The combined sources then provided an intensity, $\underline{I} = 3.0$. The procedure was repeated, adding unit increments of intensity, until resistance in excess of 1000 ohms was required for balance. A plot of the required resistance against the number of arbitrary intensity units then provided a measure of photometric linearity.

The light level and photoreceptor sensitivity varies widely for the three CIE functions so it was necessary to determine linearity for each of the three filter combinations. At the low effective light levels of the Z function the system was found to be linear, but at the higher effective light levels of the X and Y functions the slope of the response decreased somewhat with increasing light level. The best quadratic fit to the observed resistance by an equation of the form

$$\text{Resistance} = AI - BI^2$$

was calculated. The differences between the "quadratic resistance," calculated from the equation, and a "linear resistance," provided by the straight line through the origin and $\underline{I} = 3.5$ (which corresponds to about 1000 ohms resistance) were used to construct correction tables which are included as Tables V and VI in Appendix II.

PRELIMINARY EXPERIMENTAL RESULTS

Solid blue and red prints on uncoated paper (Perkins-Goodwin advertisements on the back cover of Pulp and Paper for January and June, 1974, respectively) were selected for preliminary measurements. A $BaSO_4$ compact having reflectance factors $\underline{R}_{\underline{X}(red)} = 0.987$, $\underline{R}_{\underline{Y}} = 0.986$, and $\underline{R}_{\underline{Z}} = 0.986$, as determined on the standard brightness tester at the Institute, was used for calibration. Table II contains the corresponding reflectance factors for the blue and red paper prints. The table also includes values determined with the standard brightness tester. All the values are for 45°-0° viewing conditions but, because of the much larger solid angle of both illumination and viewing of the standard brightness tester, some differences in reflectance factors may be anticipated unless the angular distribution of reflectance for the prints is identical to that of the $BaSO_4$ compact. The reflectance factors were converted to X, Y, and Z tristimulus values by the equations:

$$X = 0.9804\ (0.7988 \times R_{X(red)} + 0.2012 \times R_Z)$$

$$Y = R_Y$$

$$Z = 1.1812 \times R_Z.$$

The chromaticity coefficients, $\underline{x}$ and $\underline{y}$, were calculated by the equations:

$$x = \frac{X}{X + Y + Z}$$

$$y = \frac{Y}{X + Y + Z}.$$

Chromaticity coefficients and luminance factors ($\underline{Y}$) for both surface and internal components of reflectance and for their composite effect are presented in Table III. Similar values for the standard brightness tester are also included. It is apparent that the surface component provides 23.1 and 17.4% of the total luminance factor for the red and blue prints, respectively. The desaturating effect of the surface reflection is best appreciated by examination of the chromaticity plots shown as Fig. 5 and 6 which reveal both the near white nature of the surface component and the difference in saturation between the internal and composite chromaticities.

TABLE II

SURFACE, INTERNAL AND COMPOSITE TRISTIMULUS REFLECTANCE FACTORS OF PRINTS

	Function		
	R_X(red)	R_Y	R_Z
Red Print			
Surface component	0.060	0.054	0.044
Interior component	0.340	0.178	0.074
Composite	0.400	0.232	0.117
Standard brightness tester	0.387	0.230	0.110
Blue Print			
Surface component	0.037	0.042	0.054
Interior component	0.094	0.202	0.497
Composite	0.131	0.244	0.551
Standard brightness tester	0.125	0.241	0.545

TABLE III

SURFACE, INTERNAL AND COMPOSITE CHROMATICITIES AND LUMINANCE FACTORS OF PRINTS

	Chromaticity Coordinates		Luminance Factor
	x	y	Y, %
Red Print			
Surface component	0.339	0.337	5.36
Interior component	0.515	0.326	17.8
Composite	0.476	0.328	23.2
Standard brightness tester	0.474	0.336	23.0
Blue Print			
Surface component	0.271	0.291	4.24
Interior component	0.179	0.210	20.2
Composite	0.191	0.221	24.4
Standard brightness tester	0.188	0.221	24.1

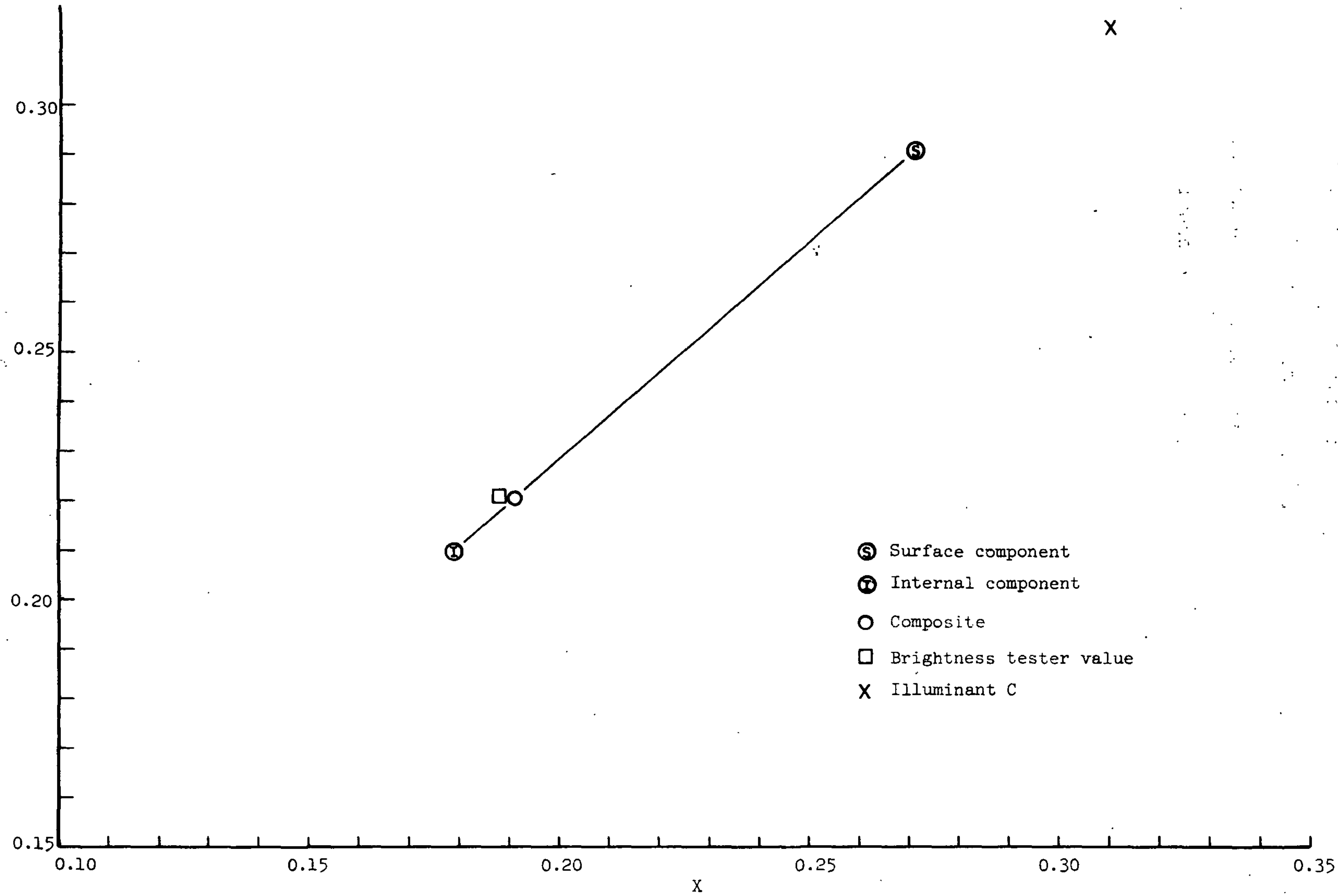

Figure 5. Chromaticity Diagram for the Blue Printed Paper

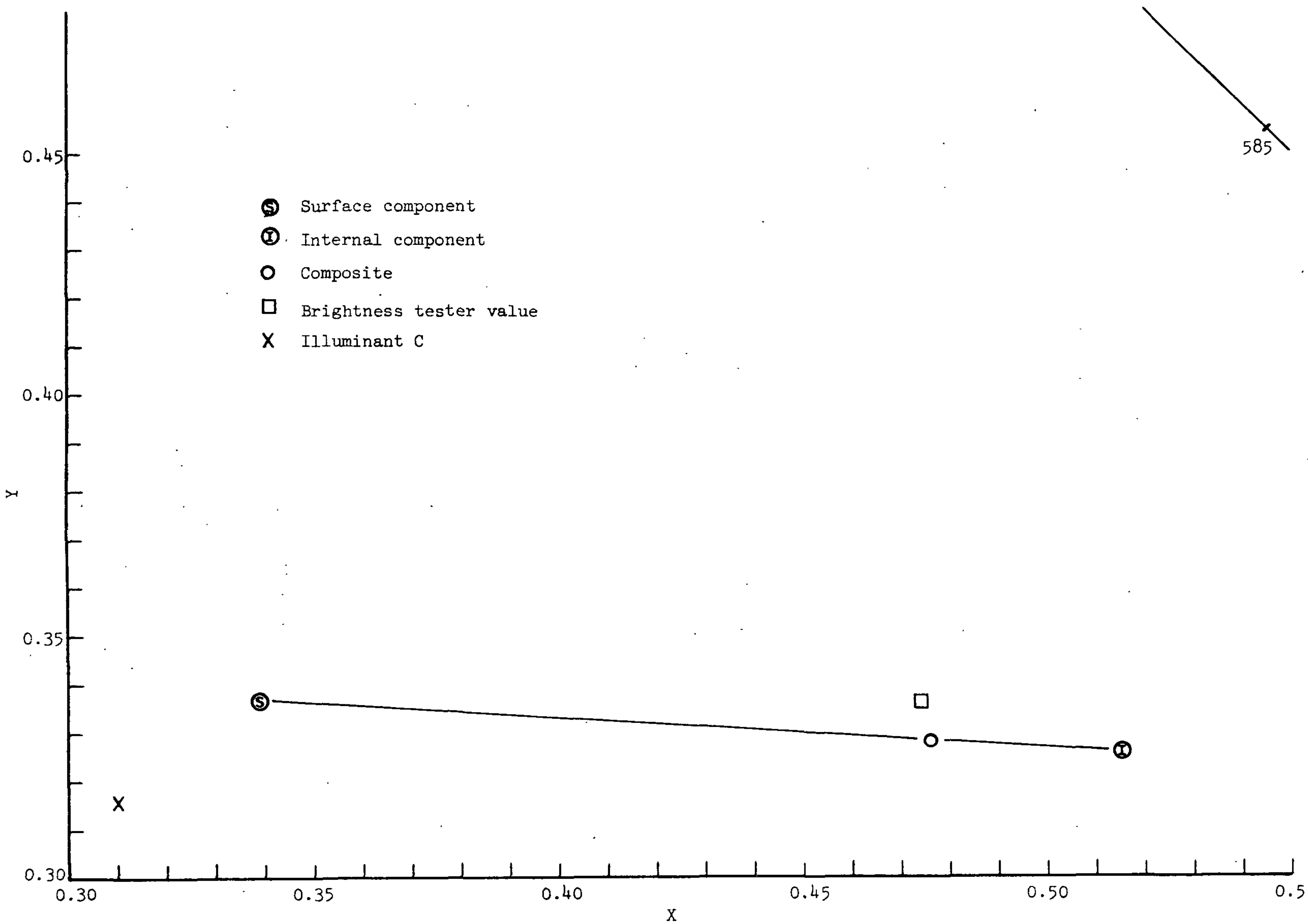

Figure 6. Chromaticity Diagram for the Red Printed Paper. The Spectrum Locus in the Vicinity of 585 nm is also Shown

DISCUSSION OF PRELIMINARY RESULTS

The results of the preliminary experiments recorded in Fig. 5 and 6 demonstrate the capability of the equipment to resolve light reflected from a printed surface into a more saturated internal component and a near white surface component. The instrument should be entirely satisfactory for the work planned for this project.

There are numerous possible explanations for the surface reflection not being entirely white. Equation (3) indicates that the specular component is sensitive to the ratio between surface roughness and wavelength. It would be surprising not to find some effect of wavelength upon the angular distribution at nonspecular angles. In the case of the blue print, where the surface reflection was bluish in color, the suggestion of Bryntse (7), that light which encounters only two or three scattering centers is not completely depolarized, may apply. Such light would be included in the surface component even though it transversed some of the ink film. In the case of the red print, where the surface reflection was yellow-orange (dominant wavelength between 580 and 585 nm), it is probable that the color was, at least in large part, due to bronzing. Bronzing is a selective surface reflection due to a higher refractive index of the pigment on the long wavelength side of the absorption band. Yellow-orange bronzing is commonly observed with red inks, particularly when printed on absorbent stocks. The yellow-orange color of the surface reflection accounts for the discrepancy between the composite chromaticity and the value determined with the standard brightness tester. The brightness tester, because of its larger angles of both illumination and viewing, should accept a larger portion of the surface reflection.

FUTURE WORK

Work is continuing on prints made with the same amount of ink on various coated and uncoated papers to determine the effect of paper on the components of printed color. It is anticipated that the elapsed time interval between printing and drying, during which ink vehicle is absorbed into the paper will be an important variable affecting the surface component. Therefore, ultraviolet curing inks are being used to permit control of this variable.

Particular attention will be given to determining the extent to which the desaturating effect of surface reflection can be limited by the surface finish of the printed surface. The extent of correlation of color saturation with conventional gloss measurements of the paper and printed surface will be determined.

ACKNOWLEDGMENTS

The assistance of Mr. Leonard Dearth and Mr. Wayne Shillcox of the Institute staff is gratefully acknowledged. They have provided valuable counsel, have provided components of the colorimetric filters, and have permitted the use of their calibration filters.

LITERATURE CITED

1. Leekley, R. M., Denzer, C. W., and Tyler, R. F., Tappi 53(4):615-21(April, 1970).

2. Depew, C. A., and Weir, R. D., Applied Optics 10(4):969-70(1971).

3. Gate, L., Windle, W., and Hine, M., Tappi 56(3):61-5(March, 1973).

4. Gate, L. F., Highman, V. M., and Hine, M. J., Papeterie 96(12):923-6 (Dec., 1974).

5. Borchers, C. H., TAGA Proceedings 1958:191-8, 216.

6. Preucil, F. M., TAGA Proceedings 1962:227-34, 268-70.

7. Bryntse, G., and Norman, B., TAPPI Fall Coating and Graphic Arts Division Week Preprint, 1975:139-47.

8. Dearth, L. R., Personal communication, 1975.

9. Van den Akker, J. A., J. Opt. Soc. Am. 33(5):257-9(May, 1943).

10. Höpert, H. J., and Loof, H., Zeitschrift für Instrumentenkunde 72(5) (1964).

THE INSTITUTE OF PAPER CHEMISTRY

Russell F. Tyler

Russell F. Tyler
Research Fellow

Robert M. Leekley

Robert M. Leekley
Senior Research Associate
Division of Natural
Materials & Systems

Approved by:

John W. Swanson

John W. Swanson, Director
Division of Natural
Materials & Systems

APPENDIX I

COLOUMETRIC DATA ON INSTRUMENT COMPONENTS

TABLE IV

COMPONENTS OF COLORIMETRIC FILTERS

Filter Designation		Transmission, %[a]	Wavelength, nm[a]
		X(red) Function	
C-500[b]	Hoya	23.8	650
C-500	Hoya	50.6	650
3-76	Corning	17.6	550
3-76	Corning	43.0	550
		Y Function	
C-500[b]	Hoya	23.8	650
4-69	Corning	45.0	700
4-69	Corning	45.0	700
4-69	Corning	44.0	700
		Z Function	
C-500[b]	Hoya	23.8	650
C-500	Hoya	23.1	650
3-73	Corning	78.5	422
5-58	Corning	48.5	447

[a]These filters have been ground to various thicknesses and are classified by transmission at the designated wavelength.

[b]Filter in the light source.

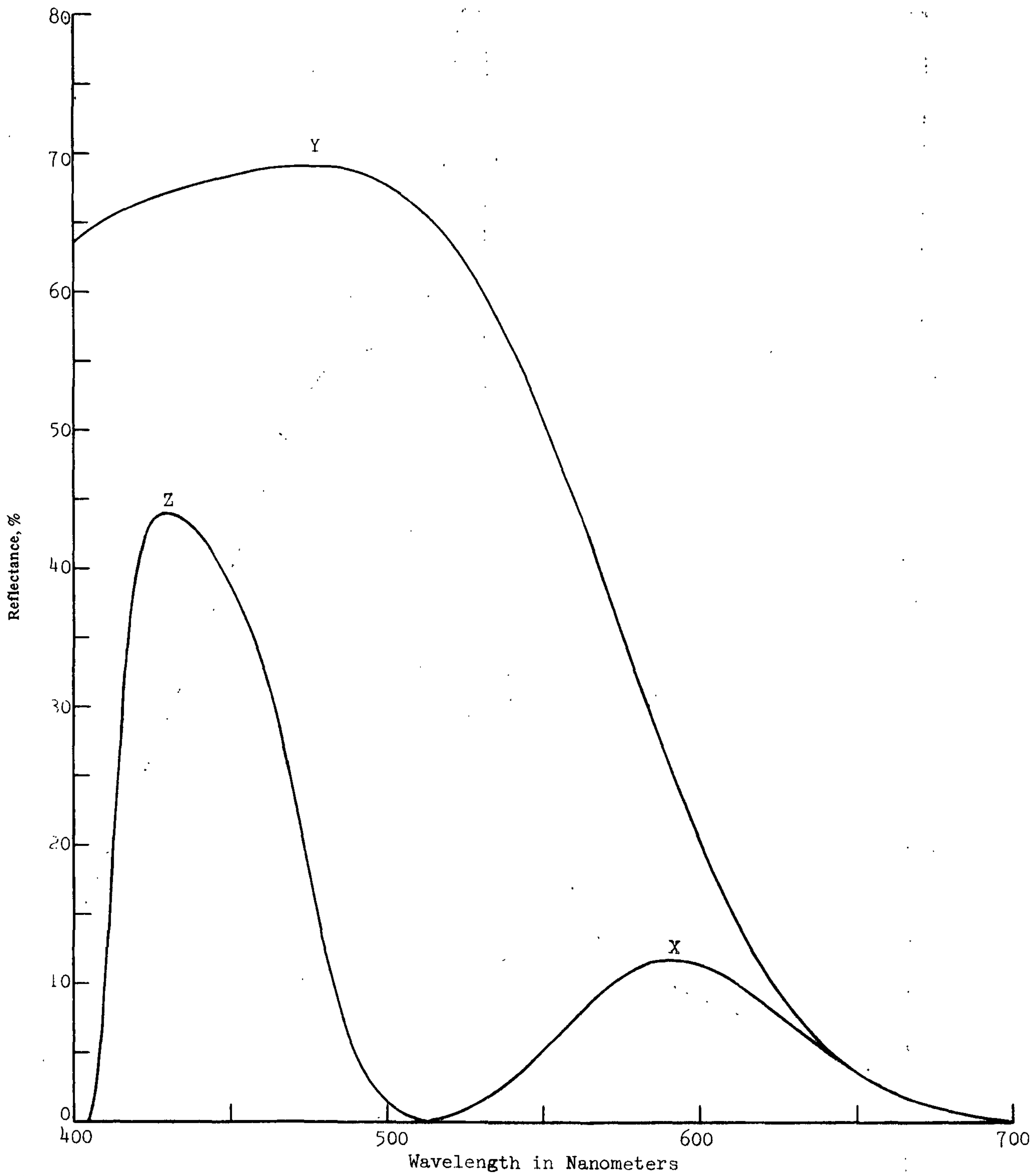

Figure 7. Spectral Transmittance of Filter Combinations Used for X(Red), Y and Z Functions

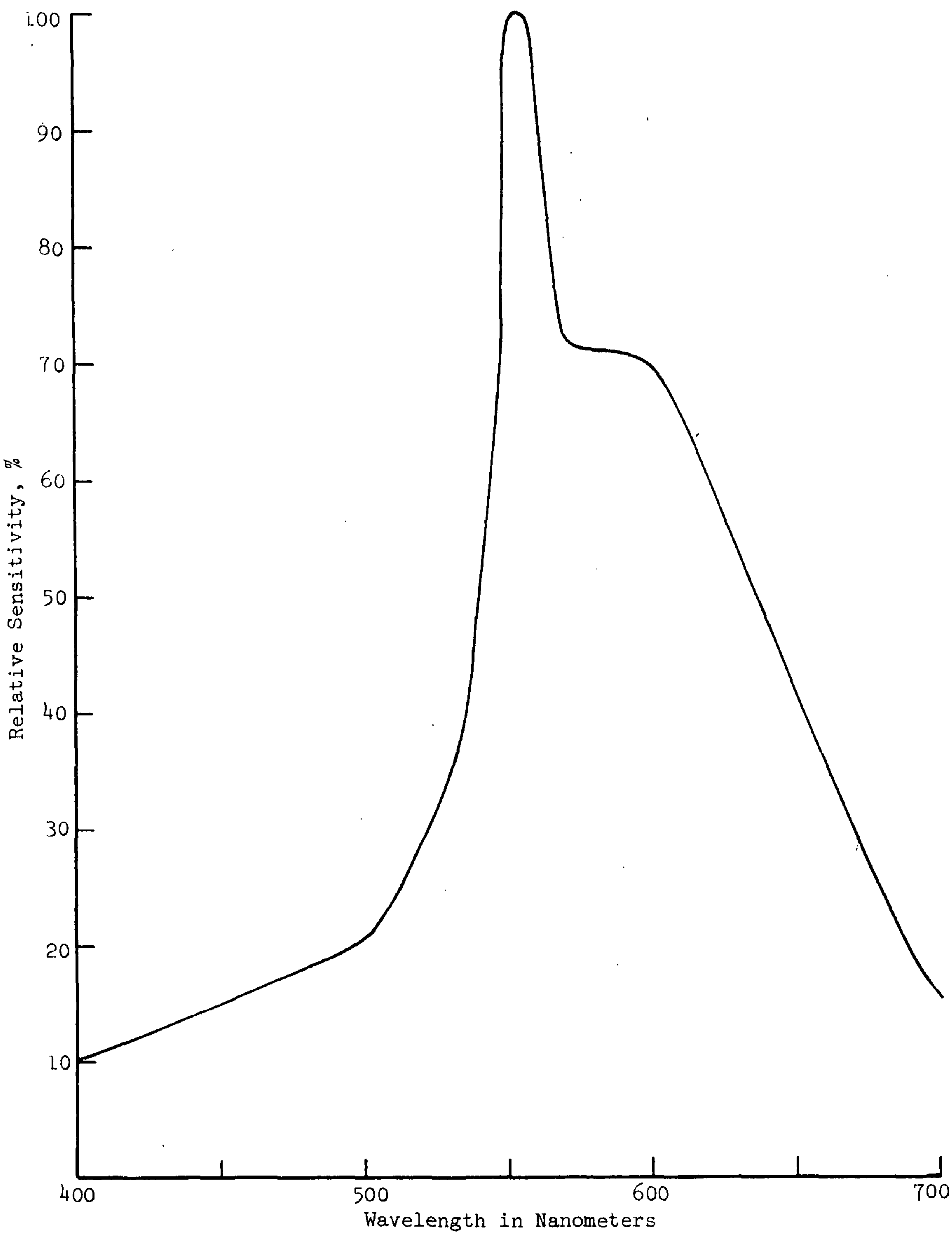

Figure 8. Relative Spectral Sensitivity of the Clairex CL505L Photoconductive Cells. Drawn from Representative Data Supplied by the Manufacturer

APPENDIX II

CORRECTION FOR PHOTOMETRIC NONLINEARITY

Light addition experiments for the Z function provided resistance values $\underline{R}_1 + \underline{R}_2$, which were linear with the light intensity, $\underline{I}$. Therefore, these values can be used directly without correction as being proportional to the intensity of the light reflected by the test specimen. However, plots of the X(red) and Y responses both decreased slightly in slope with increasing intensity and, therefore, require correction in order to obtain a numerical value which is proportional to light intensity. In each case a "quadratic resistance" of the form

$$\text{Quadratic Resistance} = AI - BI^2$$

was found to closely predict the observed resistance. For the X(red) function the equation is

$$\text{Quadratic Resistance} = 298.7939\ I - 3.8323\ I^2$$

The straight line passing through the origin and intersecting the quadratic resistance at $\underline{I} = 3.5$, was adopted as a linear "corrected resistance," proportional to light intensity.

$$\text{Corrected Resistance} = 285.3825\ I$$

Differences between quadratic resistance and corrected resistance were calculated for 10 ohm increments of quadratic resistance and used to prepare the table of corrections shown as Table V. The table gives corrections in ohms which are added to or subtracted from the observed resistance to provide a numerical value which is proportional to the intensity of light reflected by the specimen. Intermediate corrections are determined by interpolation between table values. These corrections apply when the instrument sensitivity, as determined by $\underline{R}_3 + \underline{R}_4$, corresponds to that employed in the light addition experiment, i.e., $\underline{R}_1 + \underline{R}_2$ for $BaSO_4$ at 45° incidence should be near 1000 ohms.

Table VI contains similar corrections for the Y function which were obtained in the same manner. In this case the equations are:

$$\text{Quadratic Resistance} = 307.0938\ I - 6.4270\ I^2$$

and

$$\text{Corrected Resistance} = 284.5825\ I$$

TABLE V

CORRECTIONS[a] FOR NONLINEAR RESPONSE — X(RED) FUNCTION

Observed Resistance, ohms → ↓		10	20	30	40	50	60	70	80	90
0	0.0	-0.4	-0.8	-1.3	-1.7	-2.1	-2.5	-2.9	-3.3	-3.7
100	-4.1	-4.5	-4.8	-5.2	-5.5	-5.8	-6.1	-6.4	-6.7	-7.0
200	-7.3	-7.6	-7.9	-8.1	-8.4	-8.6	-8.9	-9.1	-9.3	-9.5
300	-9.7	-9.8	-10.0	-10.2	-10.3	-10.5	-10.6	-10.8	-10.9	-11.0
400	-11.2	-11.3	-11.4	-11.5	-11.5	-11.6	-11.6	-11.7	-11.7	-11.7
500	-11.7	-11.7	-11.7	-11.7	-11.7	-11.6	-11.6	-11.5	-11.5	-11.4
600	-11.4	-11.3	-11.2	-11.1	-10.9	-10.8	-10.7	-10.5	-10.4	-10.2
700	-10.0	-9.8	-9.6	-9.4	-9.2	-9.0	-8.8	-8.5	-8.2	-8.0
800	-7.7	-7.4	-7.1	-6.8	-6.5	-6.1	-5.8	-5.5	-5.1	-4.7
900	-4.3	-3.9	-3.5	-3.1	-2.7	-2.3	-1.8	-1.4	-0.9	-0.5
1000	0.0	0.5	1.1	1.6	2.1	2.7	3.2	3.8	4.4	5.0
1100	5.6	6.2	6.8	7.4	8.1	8.7	9.4	10.0	10.7	11.5
1200	12.2	12.9	13.6	14.4	15.1	15.9	16.6	17.4	18.2	19.1
1300	19.9	20.7	21.6	22.5	23.3	24.2	25.1	26.0	26.9	27.9
1400	28.9	29.9	30.9	31.9	32.9	33.9	34.9	35.9	37.0	38.1

[a]Corrections (ohms) to be added to or subtracted from the observed resistance in order to correct for photometric nonlinearity.

TABLE VI

CORRECTIONS[a] FOR NONLINEAR RESPONSE — Y FUNCTION

Observed Resistance, ohms → ↓		10	20	30	40	50	60	70	80	90
0	0.0	-0.8	-1.5	-2.2	-2.9	-3.5	-4.2	-4.8	5.4	6.1
100	-6.7	-7.3	-7.9	-8.5	-9.0	-9.5	-10.1	-10.6	-11.1	-11.6
200	-12.1	-12.6	-13.0	-13.4	-13.8	-14.2	-14.6	-15.0	-15.3	-15.7
300	-16.0	-16.4	-16.7	-17.0	-17.3	-17.5	-17.8	-18.0	-18.3	-18.5
400	-18.7	-18.9	-19.0	-19.1	-19.2	19.3	19.4	19.5	-19.6	-19.6
500	-19.7	-19.7	-19.7	-19.7	19.7	19.6	19.6	19.5	-19.4	19.3
600	-19.2	-19.0	18.8	18.7	18.5	18.3	18.1	17.8	17.6	17.3
700	-17.0	-16.6	-16.3	-16.0	-15.6	-15.3	14.9	-14.5	-14.0	-13.6
800	-13.1	-12.6	-12.1	-11.5	-11.0	-10.5	-9.9	-9.3	-8.6	-8.0
900	-7.3	-6.7	-6.0	-5.2	-4.5	-3.7	-3.0	-2.2	-1.4	-0.6
1000	0.3	1.2	2.1	3.0	4.0	4.9	5.9	6.9	7.8	8.9
1100	10.0	11.0	12.2	13.3	14.5	15.7	16.8	18.0	19.3	20.6
1200	+22.0	23.2	24.5	25.8	27.2	28.6	30.0	31.4	32.9	34.4
1300	36.0	37.5	39.1	40.6	42.3	43.9	45.5	47.3	48.9	50.7
1400	52.5	54.4	56.2	58.0	59.9	61.8	63.7	65.6	67.6	69.6

[a]Corrections (ohms) to be added to or subtracted from the observed resistance in order to correct for photometric nonlinearity.